Increased tRNA modification and gene-specific codon usage regulate cell cycle progression during the DNA damage response

Ashish Patil[1,2,3]
Madhu Dyavaiah[1,3]
Fraulin Joseph[1, 3]
John P. Rooney[2,3,*]
Clement T. Y. Chan[4]
Peter C. Dedon[5,6]
Thomas J. Begley [1, 3†]

[1]College of Nanoscale Science and Engineering, University at Albany, SUNY, 257 Fuller Road, NFE 4905, Albany, NY 12203, [2]Department of Biomedical Sciences, [3]Cancer Research Center, University at Albany, State University of New York, Rensselaer, NY 12144, [4]Department of Chemistry [5]Department of Biological Engineering, and [6]Center for Environmental Health Sciences, Massachusetts Institute of Technology, Cambridge, MA 02139

*Present address: Nicholas School of the Environment, Duke University, Durham, NC, 27708

†corresponding author: tbegley@albany.edu

Running title: tRNA modifications change during the cell cycle

Abstract

S-phase and DNA damage promote increased ribonucleotide reductase (RNR) activity. Translation of *RNR1* has been linked to the wobble uridine modifying enzyme tRNA methyltransferase 9 (Trm9). We predicted that changes in tRNA modification would translationally regulate *RNR1* after DNA damage to promote cell cycle progression. In support, we demonstrate that the Trm9-dependent tRNA modification 5-methoxycarbonylmethyluridine (mcm^5U) is increased in hydroxyurea (HU)-induced S-phase cells, relative to G1 and G2, and that mcm^5U is one of 16 tRNA modifications whose levels oscillate during the cell cycle. Codon-reporter data matches the mcm^5U increase to Trm9 and the efficient translation of AGA codons and *RNR1*. Further, we show that in *trm9Δ* cells reduced Rnr1 protein levels cause delayed transition into S-phase after damage. Codon re-engineering of *RNR1* increased the number of *trm9Δ* cells that have transitioned into S-phase one hour after DNA damage and have increased Rnr1 protein levels, to a level similar to that of wild-type cells expressing native *RNR1*. Our data supports a model in which codon usage and tRNA modification are regulatory components of the DNA damage response, with both playing vital roles in cell cycle progression.

Key words: DNA damage response / Cell cycle / Translation / Codon usage / tRNA / Trm9

Introduction

Saccharomyces cerevisiae tRNA methyltransferase 9 (Trm9) methylates wobble uridines to facilitate the synthesis of 5-methoxycarbonylmethyluridine (mcm^5U) and 5-methoxycarbonylmethyl-2-thiouridine (mcm^5s^2U) in specific tRNAs encoding arginine, lysine, glutamine and glutamic acid.[1-3] Trm9-catalyzed tRNA modifications have been implicated in differentiating between cognate and near cognate codons in mixed codon boxes and optimizing codon-anticodon interactions.[1, 4] Reporter studies support that Trm9-catalyzed tRNA modifications enhance binding to codons ending in A and G in arginine and glutamic acid mixed codon boxes to increase the speed of translation in a codon dependent context.[3] *In vivo,* the influence of Trm9-dependent tRNA modifications on translation has been demonstrated for components of the ribonucleotide reductase (RNR) complex, with Rnr1 and Rnr3 protein deficiencies noted in asynchronous *trm9Δ* cells.[3] High throughput and targeted studies have also demonstrated that *trm9Δ* cells are sensitive to killing by ionizing radiation and alkylating agents.[3, 5-7] When taken together, the reported work on Trm9 and corresponding mutants demonstrates that there is a link between tRNA modifications, translation and the DNA damage response.

The RNR complex plays an important role in regulating cell cycle transitions and the DNA damage response. The RNR complex has four protein subunits: Rnr1, Rnr2, Rnr3 and Rnr4. It catalyzes the rate-limiting step in the biosynthesis of deoxyribonucleotides (dNTPs) from ribonucleotides,[8] with the concentration of dNTP pools limiting for DNA replication and DNA repair. During DNA replication dNTPs need to be replenished,[9, 10] thus high RNR activity is required to complete S-phase. During conditions of DNA damage, DNA replication requires a further increase in dNTP levels to promote efficient repair synthesis.[11, 12] The survival of *S. cerevisiae* in response to DNA damaging agents has been previously shown to depend on increased dNTP levels.[13]

Hence, factors that reduce dNTP levels, by reducing Rnr1, Rnr2 and Rnr4 levels or RNR activity, render cells hypersensitive to DNA damaging agents as well as to the RNR inhibitor hydroxyurea (HU).[14] DNA synthesis is highest during S-phase and is lowest during G1-phase; hence, RNR activity is tightly coupled with phases of the cell cycle.[15-18] RNR activity is restricted in the G1-phase of the cell cycle and as the cell transitions from G1 to S-phase,[19, 20] there is a sudden surge in RNR activity triggered by the phosphorylation mediated degradation of Sml1, sub-cellular re-localization of subunits and increased transcription of *RNR1* and *RNR3.*[8, 21-24]

In *S. cerevisiae,* 5-methylcytosine (m^5C) tRNA modifications are increased in response to oxidative stress,[25, 26] suggesting a dynamic role for the tRNA wobble position in regulating protein synthesis. Changes in the levels of many other tRNA modifications occur under conditions of increased reactive oxygen species, which include C_m, $m^2{}_2G$, mcm^5U, U_m and A_m modifications,[25] suggesting that global tRNA reprogramming is part of the cellular stress response. The observed increase in m^5C and mcm^5U modifications has provided strong support for the theory that the wobble position of the anticodon plays a regulatory role during stress responses. Cell cycle oscillations are tightly coupled to efficient stress and DNA damage responses; consequently timely cell cycle progression can promote efficient responses to stress. We reasoned that increased tRNA modification and translation should also have roles in the surge in RNR activity required for cells to transition from G1 to S, which should be especially prominent under conditions of DNA damage.

In the following *S. cerevisiae* based study, we demonstrate that the levels of 16 tRNA modifications oscillate during the course of the cell cycle, with a distinct collection occurring in HU-induced S-phase. HU and MMS activate the intra-S checkpoint and

increase the transcription of RNR genes to promote the DNA damage response.[27-29] We show that mcm^{5}U tRNA modification increases in HU-induced S-phase, relative to G1 and G2, to promote the codon-dependent translation of *RNR1* and boost RNR activity. Further, we demonstrate that mutants lacking Trm9 display a DNA damage-induced cell cycle phenotype characterized by delayed transition from G1- to S-phase, relative to wild-type, in response to DNA damage. Notably, we also show that a change in *RNR1* codon usage can rescue the damage-induced cell cycle phenotype associated with *trm9Δ* cells and increase Rnr1 protein levels in *trm9Δ* cells. Ultimately, our study demonstrates that *RNR1* is translationally regulated by the Trm9-dependent tRNA modification mcm^{5}U. Our study also highlights new regulatory roles for gene-specific codon usage patterns and oscillations in tRNA modifications during the cell cycle.

Results

Rnr1 protein levels are reduced in *trm9Δ* cells, relative to wild-type, during all phases of the cell cycle, with the largest difference in S-phase

We synchronized cells in G1-phase using α-factor, in S-phase using hydroxyurea and in G2-phase using nocadazole, we also treated cells with MMS for 2-hours to align them in S-phase. We then measured Rnr1 protein levels **(Figure 1A)** using immunoblots. Relative to wild-type, Rnr1 protein levels were lower in *trm9Δ* cells synchronized in G1, S, G2 and after treatment with MMS. The difference between Rnr1 levels in wild-type and *trm9Δ* cells was most extreme in HU-induced S-phase. RNR1 is known to be transcriptionally induced in S-phase,[21] which helps account for the modest G1 to S increase in Rnr1 protein levels in *trm9Δ* cells. Previously, we have used northern blots and polysome profiles to demonstrate that the transcription of *RNR1* is similar in wild-type and *trm9Δ* cells and that translation of *RNR1* is perturbed in asynchronous *trm9Δ* cells.[3] Combined, our data supports the idea that *RNR1* translation and tRNA modifications are regulated differently during the cell cycle.

tRNA modification patterns change as a function of cell cycle phase, with mcm^5U modifications increased in HU-induced S-phase

To analyze tRNA modification levels as a function of the cell cycle, wild-type cells were grown to mid-log phase and synchronized in G1, S and G2 **(Figure 1B)**, as well as treated with MMS for 2-hours. Small RNA species were isolated and tRNA modifications were quantified by LC-MS/MS analysis **(Figure 1C, Supplemental Table 1A-C)**. RNA extracted from cells treated with MMS for 2-hours was heavily degraded and not suitable for further analysis. The quantitative tRNA modification data specific to G1-, HU-induced S- and G2-phases was analyzed relative to asynchronous cells, clustered and viewed as

a heat map to identify modifications that change as a function of cell cycle stage **(Figure 1C)**. We have identified 12, 2 and 9 significant ($P < 0.05$) changes in tRNA modification levels in G1-, S-, and G2-phases of the cell cycle, respectively. In both G2 and G1, we observed significant decreases in I, m^5U, m^5C, Cm, m^7G, m^1I and m^1A modifications relative to asynchronous cells. Modifications to positions 34 (wobble base) and 37 (adjacent to the anticodon) of tRNA are well represented in this list and include m^5C, Cm, and m^1I. We were very interested in the S-phase data, as efficient DNA synthesis after DNA damage requires optimal Rnr1 protein levels in this phase and we predicted that tRNA modification levels would be distinct. We observed a significant ~2-fold increase ($P < 0.003$) in mcm^5U modifications during S-phase, relative to asynchronous, G2 or G1 cells **(Figure 1D),** with an ~2-fold reduction ($P < 0.04$) in the mcm^5s^2U modification. This could suggest that dethiolation of mcm^5s^2U is driving the increase in mcm^5U levels; however other explanations are also possible. These include increased transcription or selective degradation of specific tRNA's. Nevertheless, our results support the notion that increased mcm^5U wobble bases, which are Trm9-dependent, help promote the translation of *RNR1* to provide the burst in RNR activity needed to support DNA synthesis in S-phase after DNA damage.

Transition into S-phase is delayed in *trm9Δ* cells after DNA damage

If mcm^5U modifications increase the translation of *RNR1* in S-phase after DNA damage, then the loss of mcm^5U should lead to a DNA damage-induced cell cycle phenotype in *trm9Δ* cells. We tested our hypothesis using wild-type, *trm9Δ* and *trm9Δ* + *TRM9* cells treated with MMS, followed by propidium iodide (PI) based staining of DNA content and fluorescent activated cell sorting (FACS) to characterize cell cycle populations. We observed that 95% of the wild-type cells had progressed into S-phase

2.5-hours after treatment with 0.04% MMS, whereas 25% of *trm9Δ* cells remained in G1-phase **(Figure 2)**. We were able to alleviate the MMS-induced cell cycle phenotype in *trm9Δ* cells by re-expressing *TRM9*. Similar experiments and results were also performed and obtained using ionizing radiation and HU. We observed that 99% of the wild-type cells were outside of G1-phase 3-hours after exposure to 200 Gy of IR, whereas 20% of the *trm9Δ* cells remained in G1-phase **(Supplemental Figure 1)**. After HU treatment of *trm9Δ* cells, we also observed a delayed transition into S-phase **(Supplemental Figure 2)**, a phenotype similar to what we have described for MMS.

Our cell cycle results support the conclusion that *trm9Δ* cells transition slowly into S-phase after DNA damage, relative to wild-type. To further test our prediction, we performed cell synchronization experiments. First, wild-type and *trm9Δ* cells were synchronized in G1-phase with alpha factor treatment, washed and then cultured in YPD or YPD containing MMS. We observed that ~80% of wild-type cells transition into S-phase 30 minutes after being released into MMS **(Figure 3)**. In contrast, only ~50% of the G1 synchronized *trm9Δ* cells transition into S-phase by 30 minutes. Notably it took 3 hours after release into MMS for ~80% of the *trm9Δ* cells to have transitioned into S-phase. Cumulatively, our cell cycle results provide evidence that there is a DNA damage-induced cell cycle phenotype (*i.e.,* delayed transition into S-phase) in *trm9Δ* cells.

The delayed transition into S-phase after DNA damage observed in *trm9Δ* cells can be alleviated by increased RNR activity.

The *RNR1* transcript is upregulated in S-phase, relative to G1, and after exposure to HU or MMS.[21] Increased RNR activity is vital for S-phase and an efficient

DNA damage response. We have previously demonstrated that poor translation of *RNR1* mRNA in asynchronous *trm9* mutants leads to lower Rnr1 levels.[3] Hence, we reasoned that reduced RNR activity, via an Rnr1 deficiency, is responsible for our observed cell cycle phenotype in *trm9Δ* cells after DNA damage. We expressed *RNR1* from the *ADH1* promoter in both wild-type and *trm9Δ* cells. In theory, this could partially override the translational defect associated with deficiencies in Trm9 and provide higher levels of the *RNR1* transcript and protein in both wild-type and *trm9Δ* cells. Each of the cell types was treated with MMS and a cell cycle profile was determined over 3-hours. We observed that over-expression of *RNR1* transcripts partially alleviated the MMS-induced cell cycle phenotype and increased the number of *trm9Δ* cells that transitioned into S-phase **(Figure 4)**.

Mec1-Rad53-Dun1 dependent phosphorylation of Sml1 will promote degradation of Sml1 to provide a rapid increase in dNTP levels, with this occurring during S-phase or and after DNA damage.[22] Deletion of *SML1* has been reported to suppress the DNA damage phenotype associated with the decreased *RNR* subunit transcription.[30] In general, lower Sml1 protein levels will increase RNR activity and lead to increased dNTP levels and resistance to DNA damage induced cell death.[22] We deleted *SML1* in *trm9Δ* cells and observed increased numbers of cells outside of G1-phase in *sml1Δ-trm9Δ* cells after IR or MMS damage **(Figure 5 and Supplemental Figure 3)**, when compared to *trm9Δ* cells. Results from both our *RNR1* over-expression and *sml1Δ* experiments support the idea that low Rnr1 levels and reduced RNR activity in *trm9Δ* cells results in a delayed transition into S-phase after DNA damage.

Trm9-catalyzed tRNA modifications enhance the translation of *RNR1* in a codon-dependent fashion.

Our data on tRNA modifications, Rnr1 protein levels and cell cycle progression support the idea that increased mcm^5U levels promote the translation of *RNR1* transcripts in S-phase during the DNA damage response. The *RNR1* transcript has a distinct codon usage, characterized by over usage of AGA and GAA codons.[3] We suggest that the increase in mcm^5U tRNA modification affects translation in a codon- and thus gene-dependent fashion. To test this model, we used a dual reporter system to analyze the influence of Trm9-catalyzed modifications on the translation of 9 different codon runs. The dual reporter consists of Renilla luciferase connected in frame by an intervening 12 base pair sequence (5'-CCCGGGGAGCTC-3') to Firefly luciferase.[31] Both Renilla and Firefly Luciferase are transcribed on the same open reading frame and efficient translation of Firefly Luciferase requires efficient translation of the 12 base pair sequence (*i.e.,* 4 codon) linker region. The resulting Renilla-linker-Firefly activities are, in theory, a single protein with Renilla luciferase activity serving as an internal control. The dual Luciferase construct is under the control of an *ADH1* promoter and *CYC1* terminator (cloned in pJD375 plasmid). The Firefly/Renilla ratio is an indicator of the translational efficiency across the intervening 12 base pair (4 codon) sequence. In the test reporter plasmids, the 12 base pair intervening sequence was replaced by either 4 AGA, AGG, AAA, AAG, GAA, GAG, CAA, CAG or GGA codons in a row (designated a 4X codon run) and the reporters were individually transformed into the wild-type and *trm9Δ* cells. Each of the cells was grown to log phase and the Firefly/Renilla ratio was determined **(Figure 6A).** We observed that Trm9 significantly enhances the levels of Firefly activity associated with 4XAGA, 4XGAA and 4XCAA codon runs. In theory, the 4XAGA corresponds to mcm^5U in $tRNA^{-Arg}$, 4XGAA corresponds to mcm^5s^2U in $tRNA^{-Glu}$ and 4XCAA corresponds to mcm^5s^2U in $tRNA^{-Gln}$. The 4XAGA, 4XGAA and 4XCAA

results support the idea that Trm9-catalyzed tRNA modifications are required for the optimal translation of specific codons. In *trm9Δ* cells, we observed significantly higher Firefly activity specific to the 4XGAG and 4XTTG reporters, corresponding to glutamic acid and leucine, respectively. The increased reporter activity suggests that GAG and TTG codons were translated more efficiently in the absence of Trm9-catalyzed modifications.

AGA and TTG codons are specific to amino acids encoded by 6 codons, with 4 of these codons belonging to a family codon box. The native *RNR1* gene has many of these individual codons (18 AGA and 22 TTG) and we hypothesized that a codon-optimized *RNR1* gene that increased Rnr1 protein levels could rescue the DNA damage-induced *trm9Δ* cell cycle phenotype. To test this hypothesis, we used a codon optimized *RNR1* gene, with the goals of providing the most translatable unit and, where possible, removing codons that are regulated by Trm9-catalyzed tRNA modifications. We have previously used this codon optimized RNR1 gene (*Opt-RNR1*),[4] to support the idea that native *RNR1* transcript is susceptible to translational infidelity. *Opt-RNR1* uses all high usage codons and has all AGA and TTG codons converted to CGT and CTA, respectively. *Opt-Rnr1* replaced the endogenous *RNR1* at its native locus in both wild-type and *trm9Δ* mutants. We studied the cell cycle progression of wild-type and *trm9Δ* cells having either native or codon-optimized *RNR1* genes **(Figure 6B, Supplemental Figure 4).** We observed that *trm9Δ* cells with the codon-optimized *RNR1* had many more cells in S-phase after DNA damage, relative to *trm9Δ* cells with native *RNR1,* and had a cell cycle profile similar to wild-type cells containing the native *RNR1* gene. In contrast, *trm9Δ* cells expressing native *RNR1* had fewer cells transition to S-phase after exposure to MMS. Our cell cycle results predicted that Rnr1 protein levels would be higher in the *trm9Δ* cells expressing the codon-optimized *RNR1* gene, relative to

trm9Δ cells expressing native *RNR1*. We analyzed Rnr1 protein levels in the above-described cells (-/+ MMS) and show that, indeed, Rnr1 protein levels are higher in the *trm9Δ* cells expressing the codon optimized *RNR1* gene **(Figure 6C)**, relative to *trm9Δ* cells expressing native *RNR1*. These results support the idea that Rnr1 protein levels are regulated by gene-specific codon usage patterns and tRNA modifications during the cell cycle. They also show that tRNA modification defects can be rescued by changes in codon usage patterns. It is interesting to note that MMS-treated wild-type cells expressing the codon optimized *RNR1* transitioned more rapidly into S-phase after DNA damage and their Rnr1 protein levels were higher than wild-type cells expressing the native *RNR1* gene **(Figure 6B-C)**. These observations further support the ideas that codon usage plays a regulatory role during cell cycle progression and that Rnr1 protein levels are rate limiting in regard to transition into S-phase.

Discussion

Microarray analysis has clearly shown that transcripts can be regulated in a cell cycle-specific fashion.[32] Our data demonstrates that, similar to transcript levels, the levels of specific tRNA modifications can change as a function of cell cycle stage. This implies that translation is regulated as a function of cell cycle and we have provided the example of increased *RNR1* translation being dependent upon increased mcm^5U levels. Other transcripts rich in the AGA codons are likely to have increased translation in S-phase after DNA damage, with likely candidates being *RNR2 and RNR3* (13 and 14 AGA codons, respectively).[3] In total, we have demonstrated that levels of 16 tRNA modifications significantly change when comparing G1, G2 or HU-induced S-phase to asynchronous cells. G2 and G1 specific data accounts for 14 of these modifications and suggests that translation is distinct outside of DNA replication under damaging conditions. Clearly, codon-specific translation will have a more complicated code in G1 and G2, relative to S-phase, as many modifications are decreasing. We propose a generalized model in which particular tRNA modifications regulate the translation of specific transcripts based on codon usage patterns **(Figure 7)**. There is a dynamic aspect to our model, as individual tRNA modifications increase or decrease as a function of cellular state in order to translationally regulate codon-specific transcripts. At its simplest, translation in S-phase after DNA damage can be used to increase the levels of specific AGA-rich transcripts. This codon-specific translational regulation is used to increase the levels of Rnr1, a vital component that ensures proper cell function during DNA replication under damaging conditions. Studies addressing Trm9 are the prototype for codon-specific translational regulation because mutants are only deficient in mcm^5-based modifications at the wobble position.[4] Other *trm* mutants have pleotropic deficiencies in tRNA modification status,[25] so that defining specific rules for these systems will be difficult.

Our study also demonstrates that a reduction of Rnr1 levels in *trm9* mutants is a major contributor to the delayed transition into S-phase after DNA damage. Low Rnr1 levels, and presumably low dNTP levels, have previously been associated with a cell's failure to transition into S-phase. Rothstein and co-workers have demonstrated that when *sml1-4SA* (mutant form of Sml1 that does not undergo degradation) is overexpressed in rnr1-W688G (a strain with compromised Rnr1 activity) mutants, the cells persist in G1 and delay entry into S-phase.[33] Efficient transition into S-phase may require a burst of RNR activity. In support, Chabes and Stillman have demonstrated that constitutively high dNTP levels impede the entry of cells into S-phase by slowing down the initiation of replication.[34] They have also demonstrated a large difference in dNTP levels between G1- and S-phases, as well as an increase after DNA damage. Our observations with *trm9Δ* cells are in line with these published results. The fact that we can partially rescue the cell cycle phenotype in *trm9Δ* mutants by increasing the levels of the *RNR1* transcript or Rnr1 protein by genetic means is further proof that RNR activity and dNTP levels are key determinants influencing transition into S-phase. In addition, we have identified *trm9Δ* mutants as a novel model for studying decreased RNR activity.

Our observation that Trm9-dependent tRNA modifications play an important role in promoting transition into S-phase also demonstrates another layer of regulation for cellular RNR activity. We alluded to translational regulation for Rnr1 and Rnr3 in our previous work,[3] but we failed to show increased tRNA modification levels one hour after MMS induced DNA damage. Most likely, this was because many cells are still in G1-phase one hour after MMS treatment **(Figure 2)**. Our current study demonstrates that mcm^5U modification levels increase in DNA damage associated S-phase, relative to G1 and G2, with Trm9 activity being required for a translation-based regulatory boost. RNR

activity is thus regulated transcriptionally, translationally, post-translationally and by sub-cellular localization. The correlation of tRNA modification defects with cell cycle phenotypes is not without precedent. In *S. cerevisiae*, other proteins involved in generating mcm^5-based modifications, including Trm112, Sit4 and Sap185/190, are linked to G1 to S cell cycle transition phenotypes.[35-38] Additionally, the *sit4* mutants have been shown to be sensitive to the DNA damaging agents MMS[39] and doxorubicin (SGD database). We predict that these enzymes also play roles in the translational regulation of *RNR1* or other important cell cycle genes. It is important to note that other components of the DNA damage response have been linked to tRNA. Mec1- and Rad53-signaling through Los1 is required for the accumulation of unspliced tRNA in the nucleus and subsequent delay in transition for G1 to S-phase after DNA damage.[40] Cumulatively there is much evidence to link tRNA biology to cell cycle progression after DNA damage.

We note that studies of yeast Trm9 should help elucidate the regulatory role for mammalian proteins, as the mouse and human ALKBH8 gene products are homologous to yeast Trm9.[41] ALKBH8 is a tRNA methyltransferase that can produce mcm^5U modifications, among others, and *ALKBH8* has been demonstrated to be transcriptionally up-regulated in an ATM-dependent fashion after DNA damage.[7] We suggest that dynamic changes in tRNA modifications will also occur in humans after DNA damage and that increased tRNA modification should be downstream of ATM activation. This implies that there will be translational regulation of specific transcripts after DNA damage, where changes in tRNA modification levels influence the translation of specific codons. This, in turn, influences the levels of specific proteins, via a gene-specific translational regulatory mechanism. We have observed both positive (AGA, GAA and CAA) and negative (GAG and TTG) regulation of codon runs by Trm9. While

we have primarily concentrated on the increased translation of specific transcripts by wobble base modifications, we cannot ignore the possibility that a Trm9-dependent decrease in the translation of codon specific transcripts could also occur. Reduced or restricted translation of specific codon usage patterns by a given tRNA modification may be a way to decrease the levels of proteins detrimental to a biological process; however, this idea is merely speculative. Our model **(Fig. 7)** begs the question of why cells would regulate translation using codon usage and changes in tRNA modification status. One possible reason is the need for cells to quickly respond to a given cellular state. A rapid change in the level of tRNA modifications would allow cells to use existing transcripts more or less efficiently and this could provide a vital cellular response to stress or changes in environmental conditions.

Materials and methods

Yeast and growth conditions

Supplemental tables 2 & 3 list the *S. cerevisiae* strains and the oligonucleotides used in the study. The *trm9Δ* mutants were made by transforming a *URA3* knock out cassette derived from a *trm9Δ* heterozygous mutant (YSC4427-98798995) from Open Biosystems [Huntsville, AL]. Mutants were selected on SD–Ura plates and were confirmed by PCR. Media preparation and other yeast manipulations were performed using standard methods.[42] The *sml1Δ* cells were generated using the corresponding *KanMX* cassette derived from the *S. cerevisiae* Gene Deletion library. The *RNR1* gene was cloned by PCR based approaches in pHybcl/HK (Invitrogen; Carlsbad, CA) using *Sac*I and *SalI* cloning sites. The generated plasmid, pHybcl/HK-*RNR1*, has the *RNR1* gene under the control of the *ADH1* promoter and *ADH1* transcription terminator. It was transformed into cells and selected for on SD-His plates.

Western blots

Wild-type and *trm9Δ* cells were grown to ~5 X 10^6 cells/ml in YPD and treated as described in figure legend 1. Protein extracts were prepared as described,[3] and protein concentrations were measured using a BCA Protein Assay Kit (Pierce, Rockford, IL). Western blots were performed as described [3] using anti-tap rabbit pAB and stabilized goat anti-rabbit HRP conjugate secondary (Thermo Scientific; Rockford, IL) and rabbit pAB to β-tubulin (Abcam; Cambridge, MA).

Flow cytometric analysis

Cells were grown to ~1 X 10^7 cells/ml in YPD and treated as described in the legend. Chemicals included MMS (Sigma-Aldrich; St. Louis, MO), nocadazole (Sigma-Aldrich; St. Louis, MO), α-factor (Zymo Research; Irvine, CA) and hydroxyurea (MP

Biomedical; Solon, OH). Samples were spun down immediately and fixed overnight in 75% ethanol. Fixed cells were spun down and washed twice with distilled water. Cells were re-suspended in 1 ml of 50 mM sodium citrate pH 7.0 and 80 μg of RNAse A (Fisher Bioreagents; Fair Lawn, NJ) was added. Samples were then incubated for 1 hour at 55° C and then 250 μg of Proteinase K (Amresco; Solon, OH) was added to each sample, followed by incubation for 1 hour at 55° C. DNA staining was facilitated by the addition of 20 mg/ml propidium iodide (Sigma-Aldrich; St. Louis, MO) to each sample, followed by a 30 minute incubation at room temperature. DNA content was analyzed using a BD LSRII flow cytometer. Histograms depicting cell cycle state were generated using WinMDI 2.8 software (Scripps Research Institute) and the percentage of cells in G1-phase was calculated using ModFit LT 3.2 software (Verity Software House; Topsham, ME).

Relative quantification of secondary modifications on tRNA

Cells were arrested in G1, S and G2 or asynchronously grown as described above. Modified ribonucleosides in tRNA were identified and quantified as reported previously.[25] Cells were suspended in 1.5 ml of Trizol reagent with deaminase inhibitors (5 mg/mL coformycin, 50 μg/ml tetrahydrouridine) and antioxidants (0.1 mM deferoxamine mesylate, 0.5 mM butylated hydroxytoluene) to prevent nucleoside modification artifacts,[43, 44] *S. cerevisiae* cell pellets were lysed by 3 cycles of bead beating in a Thermo FP120 Bead Beater set at 6.5 m/s for each 20 s cycle, with 1 min of cooling on ice between cycles. Lysates were extracted with 0.3 ml volume of chloroform at ambient temperature for 5 minutes, with 3 minutes of phase separation. The solutions were centrifuged at 12,000 X g for 15 min at 4 °C and the aqueous phase was collected. Absolute ethanol was added to the aqueous phase (35% v/v) and small RNA species

were then isolated using the PureLink miRNA Isolation Kit according to manufacturer's instructions. The quality and concentration of the resulting small RNA mixture was assessed with a Bioanalyzer (Agilent Small RNA Kit), with tRNA comprising >95% of the small RNA species present in the mixture. Following the addition of deaminase inhibitors, antioxidants and $[^{15}N]_5$-2'-deoxyadenosine internal standard (6 pmol), tRNA (6 μg) in 30 mM sodium acetate and 2 mM $ZnCl_2$ (pH 6.8) were hydrolyzed with nuclease P1 (1 U) and RNase A (5 U) for 3 hours at 37°C. The resulting products were dephosphorylated with alkaline phosphatase (10 U) and phosphodiesterase I (0.5 U) for 1 hour at 37°C following the addition of acetate buffer to 30 mM, pH 7.8. The enzymes were removed by filtration (Microcon YM-10). Ribonucleosides were resolved on a Thermo Scientific Hypersil GOLD aQ reverse-phase column (150 X 2.1 mm, 3 μm particle size) eluted with the following gradient of acetonitrile in 8 mM ammonium acetate at a flow rate of 0.3 ml/min and 36 °C: 0–18 min, 0–1%; 18–23 min, 1%; 23–28 min, 1–6%; 28–30 min, 6%; 30–31 min, 6–100%; 31–41 min, 100%. The HPLC column was coupled to an Agilent 6410 Triple Quadrupole LC/MS mass spectrometer with an electrospray ionization source operated in positive ion mode with the following parameters for voltages and source gas: gas temperature, 350 °C; gas flow, 10 L/min; nebulizer, 20 psi; and capillary voltage, 3500 V. The first and third quadrupoles (Q1 and Q3) were fixed to unit resolution and the modifications were quantified by pre-determined molecular transitions. Q1 was set to transmit the parent ribonucleoside ions and Q3 was set to monitor the deglycosylated product ions, except for Y for which the stable C-C glycosidic bond led to fragmentation of the ribose ring; we used the m/z 125 ion for quantification. The dwell time for each ribonucleoside was 200 ms. The retention time, m/z of the transmitted parent ion, m/z of the monitored product ion, fragmentor voltage, and collision energy of each modified nucleoside and ^{15}N-labeled internal standard are as follow: D, 1.9 min, m/z 247→115, 80 V, 5 V; Y, 2.5 min, m/z 245→125,

80 V, 10 V; m^5C, 3.3 min, m/z 258→126, 80 V, 8 V; Cm, 3.6 min, m/z 258→112, 80 V, 8 V; m^5U, 4.2 min, m/z 259→127, 80 V, 7 V; ncm^5U, 4.3 min, m/z 302→170, 90 V, 7 V; ac^4C, 4.4 min, m/z 286→154, 80 V, 6 V; m^3C, 4.4 min, m/z 258→126, 80 V, 8 V; Um, 5.1 min, m/z 259→113, 80 V, 7 V; m^7G, 5.1 min, m/z 298→166, 90 V, 10 V; m^1A, 5.7 min, m/z 282→150, 100 V, 16 V; mcm^5U, 6.4 min, m/z 317→185, 90 V, 7 V; m^1I, 7.3 min, m/z 283→151, 80 V, 10 V; Gm, 8.0 min, m/z 298→152, 80 V, 7 V; m^1G, 8.3 min, m/z 298→166, 90 V, 10 V; m^2G, 9.4 min, m/z 298→166, 90 V, 10 V; I, 10.9 min, m/z 269→137, 80 V, 10 V; mcm^5s^2U, 14.2 min, m/z 333→201, 90 V, 7 V; $[^{15}N]_5$-dA, 14.4 min, m/z 257→141, 90 V, 10 V; $m^2{}_2G$, 15.9 min, m/z 312→180, 100 V, 8 V; t^6A, 17.2 min, m/z 413→281, 100 V, 9 V; Am, 19 min, m/z 282→136, 100 V, 15 V; yW, 34.2 min, m/z 509→377, 120 V, 10 V, and i^6A, 34.4 min, m/z 336→204, 120 V, 17 V. Signal intensity of each ribonucleoside was normalized with the signal intensity of $[^{15}N]_5$-dA from its sample before being analyzed with hierarchical clustering with the software Cluster 3.0, in which the ratios of modification levels in treated cells relative to untreated cells were transformed to $\log_2$ scale and were clustered using the Pearson correlation algorithm. The results were presented as a heat map using Java Treeview.

Reporter assay codon specific translation

Wild type and *trm9Δ* cells were transformed with reporter plasmids derived from pJD375 (having a 4X codon run in between Renilla and Firefly luciferase).[31] Transformed yeast cells were grown overnight in SD-Ura, then diluted into fresh YPD to ~1 × 10^6 cells/ml and grown to ~ 10^7 cells/ml. Cells were pelleted, washed twice with 0.5 ml of cold lysis buffer containing 1 mM PMSF (Pierce; Rockford, IL), then resuspended in cold lysis buffer and broken by agitation with glass beads (0.5 mm Sigma-Aldrich; ST Louis, MO). Lysates were clarified by centrifugation and supernatants were transferred to pre-chilled

tubes. Luminescence reactions were initiated by the addition of 50 µl of Promega DLR (Promega; Madison, WI) to 5 µl of clarified cell lysates and measured using a Victor Plate Reader (PerkinElmer; Waltham, MA).

RNR1 codon optimization

A codon optimized *RNR1* gene (*Opt-RNR1*) was developed computationally and was chemically synthesized by GeneScript (Piscataway, NJ), as previously described.[4] *Opt-RNR1* was cloned into pRS413 using a *SacI* (2178) to *XhoI* (2091) ligation strategy. The *RNR1* constructs along with the *HIScx* marker from pRS413 were than PCR amplified using primers that containing 40 base pairs of homology to the upstream or downstream regions of the native *RNR1* locus. Transformants were selected for their ability to grow on media lacking histidine and the presence of the insert was verified by PCR.

Acknowledgments

Financial support was provided by the National Institute of Environmental Health Sciences (R01 ES015037, R01 ES017010 and P30 ES002109), the MIT Westaway Fund and the Singapore-MIT Alliance for Research and Technology.

Author Contributions

Ashish Patil helped design the experiments, constructed strains, performed damage-induced cell cycle studies and some of the western blots. He also analyzed the data and helped write the original manuscript.

Madhu Dyavaiah contributed to experimental design, performed western blot experiments and some cell cycle experiments.

Fraulin Joseph performed western blot experiments and some cell cycle experiments.

John Rooney performed some western blot experiments.

Clement Chan measured tRNA modification levels, contributed to experimental design and helped write the manuscript.

Peter Dedon contributed to experimental design, data analysis, discussed results and helped write the manuscript.

Thomas Begley contributed to experimental design, data analysis, discussed results and helped write the manuscript.

Conflicts of Interest

The authors report no conflicts of interest.

References

1. Kalhor HR, Clarke S. Novel methyltransferase for modified uridine residues at the wobble position of tRNA. Mol Cell Biol 2003; 23:9283-92.

2. Lu J, Huang B, Esberg A, Johansson MJ, Bystrom AS. The Kluyveromyces lactis gamma-toxin targets tRNA anticodons. RNA 2005; 11:1648-54.

3. Begley U, Dyavaiah M, Patil A, Rooney JP, DiRenzo D, Young CM, et al. Trm9-catalyzed tRNA modifications link translation to the DNA damage response. Mol Cell 2007; 28:860-70.

4. Patil A, Chan CT, Dyavaiah M, Rooney JP, Dedon PC, Begley TJ. Translational infidelity-induced protein stress results from a deficiency in Trm9-catalyzed tRNA modifications. RNA Biology 2012; in press.

5. Bennett CB, Lewis LK, Karthikeyan G, Lobachev KS, Jin YH, Sterling JF, et al. Genes required for ionizing radiation resistance in yeast. Nat Genet 2001; 29:426-34.

6. Begley TJ, Rosenbach AS, Ideker T, Samson LD. Damage Recovery Pathways in Saccharomyces cerevisiae Revealed by Genomic Phenotyping and Interactome Mapping1 1 NIH Grants RO1-CA-55042 and P30-ES02109; NIH Training Grant ES07155 and National Research Service Award F32-ES11733 (to T.J.B.). Molecular Cancer Research 2002; 1:103-12.

7. Fu D, Brophy JAN, Chan CTY, Atmore KA, Begley U, Paules RS, et al. Human AlkB Homolog ABH8 Is a tRNA Methyltransferase Required for Wobble Uridine Modification and DNA Damage Survival. Mol Cell Biol 2010; 30:2449-59.

8. Yao R, Zhang Z, An X, Bucci B, Perlstein DL, Stubbe J, et al. Subcellular localization of yeast ribonucleotide reductase regulated by the DNA replication and damage checkpoint pathways. Proceedings of the National Academy of Sciences of the United States of America 2003; 100:6628-33.

9. Nordman J, Wright A. The relationship between dNTP pool levels and mutagenesis in an Escherichia coli NDP kinase mutant. Proceedings of the National Academy of Sciences 2008; 105:10197-202.

10. Bochner BR, Ames BN. Complete analysis of cellular nucleotides by two-dimensional thin layer chromatography. J Biol Chem 1982; 257:9759-69.

11. KoÃ§ A, Wheeler LJ, Mathews CK, Merrill GF. Hydroxyurea Arrests DNA Replication by a Mechanism That Preserves Basal dNTP Pools. Journal of Biological Chemistry 2004; 279:223-30.

12. HÃ¥kansson P, Hofer A, Thelander L. Regulation of Mammalian Ribonucleotide Reduction and dNTP Pools after DNA Damage and in Resting Cells. Journal of Biological Chemistry 2006; 281:7834-41.

13. Chabes A, Georgieva B, Domkin V, Zhao X, Rothstein R, Thelander L. Survival of DNA damage in yeast directly depends on increased dNTP levels allowed by relaxed feedback inhibition of ribonucleotide reductase. Cell 2003; 112:391-401.

14. Mulder KW, Winkler GS, Timmers HTM. DNA damage and replication stress induced transcription of RNR genes is dependent on the Ccr4â€“Not complex. Nucleic Acids Research 2005; 33:6384-92.

15. Turner MK, Abrams R, Lieberman I. Levels of Ribonucleotide Reductase Activity during the Division Cycle of the L Cell. Journal of Biological Chemistry 1968; 243:3725-8.

16. Elford HL, Freese M, Passamani E, Morris HP. Ribonucleotide Reductase and Cell Proliferation. Journal of Biological Chemistry 1970; 245:5228-33.

17. NordenskjÃ¶ld BA, Skoog L, Brown NC, Reichard P. Deoxyribonucleotide Pools and Deoxyribonucleic Acid Synthesis in Cultured Mouse Embryo Cells. Journal of Biological Chemistry 1970; 245:5360-8.

18. Elledge SJ, Zhou Z, Allen JB. Ribonucleotide reductase: regulation, regulation, regulation. Trends in Biochemical Sciences 1992; 17:119-23.

19. Elledge SJ, Zhou Z, Allen JB, Navas TA. DNA damage and cell cycle regulation of ribonucleotide reductase. Bioessays 1993; 15:333-9.

20. Horak CE, Luscombe NM, Qian J, Bertone P, Piccirrillo S, Gerstein M, et al. Complex transcriptional circuitry at the G1/S transition in Saccharomyces cerevisiae. Genes & Development 2002; 16:3017-33.

21. Elledge SJ, Davis RW. Two genes differentially regulated in the cell cycle and by DNA-damaging agents encode alternative regulatory subunits of ribonucleotide reductase. Genes Dev 1990; 4:740-51.

22. Zhao X, Rothstein R. The Dun1 checkpoint kinase phosphorylates and regulates the ribonucleotide reductase inhibitor Sml1. Proc Natl Acad Sci U S A 2002; 99:3746-51.

23. Huang M, Zhou Z, Elledge SJ. The DNA Replication and Damage Checkpoint Pathways Induce Transcription by Inhibition of the Crt1 Repressor. Cell 1998; 94:595-605.

24. Niida H, Shimada M, Murakami H, Nakanishi M. Mechanisms of dNTP supply that play an essential role in maintaining genome integrity in eukaryotic cells. Cancer Science 2010; 101:2505-9.

25. Chan CTY, Dyavaiah M, DeMott MS, Taghizadeh K, Dedon PC, Begley TJ. A Quantitative Systems Approach Reveals Dynamic Control of tRNA Modifications during Cellular Stress. PLoS Genet 2010; 6:e1001247.

26. Chan CTY, Pang YLJ, Deng W, Babu IR, Dyavaiah M, Begley TJ, et al. Reprogramming of tRNA modifications controls the oxidative stress response by codon-biased translation of proteins. Nat Commun 2012; 3:937.

27. Paulovich AG, Hartwell LH. A checkpoint regulates the rate of progression through S phase in S. cerevisiae in response to DNA damage. Cell 1995; 82:841-7.

28. Paulovich AG, Margulies RU, Garvik BM, Hartwell LH. RAD9, RAD17, and RAD24 are required for S phase regulation in Saccharomyces cerevisiae in response to DNA damage. Genetics 1997; 145:45-62.

29. Shimada K, Pasero P, Gasser SM. ORC and the intra-S-phase checkpoint: a threshold regulates Rad53p activation in S phase. Genes Dev 2002; 16:3236-52.

30. Chen SH, Smolka MB, Zhou H. Mechanism of Dun1 activation by Rad53 phosphorylation in Saccharomyces cerevisiae. J Biol Chem 2007; 282:986-95.

31. Harger JW, Dinman JD. An in vivo dual-luciferase assay system for studying translational recoding in the yeast Saccharomyces cerevisiae. RNA 2003; 9:1019-24.

32. Spellman PT, Sherlock G, Zhang MQ, Iyer VR, Anders K, Eisen MB, et al. Comprehensive identification of cell cycle-regulated genes of the yeast Saccharomyces cerevisiae by microarray hybridization. Mol Biol Cell 1998; 9:3273-97.

33. Andreson BL, Gupta A, Georgieva BP, Rothstein R. The ribonucleotide reductase inhibitor, Sml1, is sequentially phosphorylated, ubiquitylated and degraded in response to DNA damage. Nucl Acids Res 2010:gkq552.

34. Chabes A, Stillman B. Constitutively high dNTP concentration inhibits cell cycle progression and the DNA damage checkpoint in yeast Saccharomyces cerevisiae. Proc Natl Acad Sci U S A 2007; 104:1183-8.

35. Sutton A, Immanuel D, Arndt KT. The SIT4 protein phosphatase functions in late G1 for progression into S phase. Mol Cell Biol 1991; 11:2133-48.

36. Luke MM, Della Seta F, Di Como CJ, Sugimoto H, Kobayashi R, Arndt KT. The SAP, a new family of proteins, associate and function positively with the SIT4 phosphatase. Mol Cell Biol 1996; 16:2744-55.

37. Yu L, Castillo LP, Mnaimneh S, Hughes TR, Brown GW. A Survey of Essential Gene Function in the Yeast Cell Division Cycle. Mol Biol Cell 2006; 17:4736-47.

38. Jablonowski D, Schaffrath R. Zymocin, a composite chitinase and tRNase killer toxin from yeast. Biochemical Society Transactions 2007; 035:1533-7.

39. Chang M, Bellaoui M, Boone C, Brown GW. A genome-wide screen for methyl methanesulfonate-sensitive mutants reveals genes required for S phase progression in the presence of DNA damage. Proceedings of the National Academy of Sciences of the United States of America 2002; 99:16934-9.

40. Ghavidel A, Kislinger T, Pogoutse O, Sopko R, Jurisica I, Emili A. Impaired tRNA nuclear export links DNA damage and cell-cycle checkpoint. Cell 2007; 131:915-26.

41. Songe-Moller L, van den Born E, Leihne V, Vagbo CB, Kristoffersen T, Krokan HE, et al. Mammalian ALKBH8 possesses tRNA methyltransferase activity required for

the biogenesis of multiple wobble uridine modifications implicated in translational decoding. Mol Cell Biol 2010; 30:1814-27.

42. Guide to yeast genetics and molecular biology. Methods Enzymol 1991; 194:1-863.

43. Pang B, Zhou X, Yu H, Dong M, Taghizadeh K, Wishnok JS, et al. Lipid peroxidation dominates the chemistry of DNA adducts formation in a mouse model of inflammation. Carcinogenesis 2007; in press.

44. Taghizadeh K, McFaline JL, Pang B, Sullivan M, Dong M, Plummer E, et al. Quantification of DNA damage products resulting from deamination, oxidation and reaction with products of lipid peroxidation by liquid chromatography isotope dilution tandem mass spectrometry. Nat Protoc 2008; 3:1287-98.

Figure Legends

Figure 1. Rnr1 protein levels are lower in all phases of cell cycle in *trm9Δ* cells, with the largest differential observed in S-phase.

(A) Rnr1-Tap tagged strains in *TRM9* or *trm9Δ* backgrounds were grown and treated with either 5 µg/ml of alpha factor for 150 minutes, 18 mg/ml of HU for 3 hours, 0.04% MMS for 1 hour or with 5 µg/ml of nocadazole for 2-hours. The cells were spun down, the proteins extracted and a western blot was performed using anti-Tap and anti-tubulin antibodies (N = 3), with a representative blot displayed. **(B)** Wild-type (By4741) cells were synchronized in G1, S and G2 phases as described in panel A. Cell cycle profiles for asynchronous (blue) and treated (red) cells were then determined and analyzed using FlowJo Analysis Software. **(C)** The $\log_2$-based fold change for each modification in each stage of the cell cycle is reported relative to asynchronous cells in the heat map. Statistical significance for each modification change in each phase of the cell, relative to asynchronous cells, is reported in supplemental table 1. **(D)** A T-test comparison (N = 3) of the levels of mcm^5U in wild-type cells from cells in G1, S or G2-phases of the cell cycle. For C-D, LC-MS/MS was used to identify and quantitate the levels of each of 23 tRNA modifications in G1, S, G2 and asynchronous cells.

Figure 2. Trm9-catalyzed tRNA modifications promote cell cycle progression after DNA damage.

(A) Wild-type, **(B)** *trm9Δ* and **(C)** *trm9Δ* + *TRM9* cells were grown to mid-log phase and exposed to 0.04% MMS. Cell cycle profiles were then determined over 4 hours. **(D)** The percentage of wild-type (closed squares), *trm9Δ* (closed triangles) and *trm9Δ* + *TRM9* (open triangles) cells with G1 character, as defined by DNA content, after exposure to 0.04% MMS was determined using ModFit LT 3.2 software. The average of three replicates is shown, with error bars displayed in supplemental figure 5.

Figure 3. G1-synchronized *trm9Δ* cells have a delayed transition into S-phase after DNA damage.

Wild-type and *trm9Δ* cells were grown to 10^7 cells/ml and synchronized in G1 with α-factor. Cells were then released into **(A & C)** YPD or **(B & D)** YPD + MMS and cell cycle profiles were determined throughout a period of 3 hours. **(E)** The percentage of cells in G1, as determined by DNA content, was determined for wild-type (open squares) and *trm9Δ* cells (open triangles) released into YPD, as well as for wild-type (closed squares) and *trm9Δ* cells (closed triangles) released in MMS containing media. The average of 3 replicates is shown, with error bars displayed in supplemental figure 6.

Figure 4. The delayed transition into S-phase observed in *trm9Δ* cells after damage is partially rescued by *RNR1* expression. **(A)** Wild-type **(B)** *trm9Δ*, **(C)** Wild-type + *RNR1* and **(D)** *trm9Δ* + *RNR1* cells were grown to mid-log phase in YPD, exposed to 0.04% MMS and then cell cycle profiles were determined over 4 hours. **(E)** The percentage of wild-type (closed squares), *trm9Δ* (open triangles), wild-type + *RNR1* (closed diamonds) and *trm9Δ* + *RNR1* (open diamonds) cells in G1 was determined by DNA content using ModFit LT 3.2 software. The average of 3 replicates is shown, with error bars displayed in supplemental figure 7.

Figure 5. The damage-induced cell cycle delay in *trm9Δ* cells is partially rescued by *SML1* deletion. **(A)** Wild-type, **(B)** *trm9Δ,* **(C)** *sml1Δ* and **(D)** *sml1Δ– trm9Δ* cells

were grown to mid-log phase in YPD, exposed to 200 Gy IR in liquid media after which the cell cycle profiles were determined over 4 hours. **(E)** The percentage of wild-type (closed squares), *trm9Δ* (closed triangles), *sml1Δ* (open squares) and *trm9Δ-sml1Δ* (open triangles) cells in G1, as determined by DNA content, was identified using ModFit LT 3.2 software. The average of 3 replicates is shown, with error bars displayed in supplemental figure 8.

Figure 6. Trm9-catalyzed tRNA modifications affect specific codons to influence transition into S-phase after DNA damage and Rnr1 protein levels.

(A) Dual luciferase reporter (Firefly / Renilla) experiments, using 4X codons cloned in the linker region before Firefly luciferase, were performed in wild-type and *trm9Δ* cells (N = 3). P-values < 0.001 (*) or < 0.05(**) are marked. **(B)** Cell cycle analysis of MMS treated wild-type (open squares) and *trm9Δ* cells (open triangles) was performed as described above. In addition, a codon-optimized variant of *RNR1 (Opt-RNR1)* was cloned into the *RNR1* locus to produce wild-type-Opt-*RNR1* (closed squares) and *trm9Δ-Opt-RNR1* (closed triangles) cells that were then used in cell cycle studies to follow their progression after MMS damage (N =3, error bars represent standard deviations). Cell cycle traces are found in supplemental figure 9. **(C)** Wild-type and *trm9Δ* cells (containing native *RNR1* or the codon optimized version *Opt-RNR1*) were grown to ~5 X 10^6 cells/ml and were then left untreated or exposed to 0.04% MMS for one hour. Proteins were extracted and western blots were performed using anti-Rnr1 and anti-tubulin antibodies (N = 3, with a representative blot displayed).

Figure 7. Model for how tRNA modifications regulate the transition into S-phase after DNA damage.

The reprogramming of tRNA modifications during DNA replication under damaging conditions is used to increase the translation of the AGA rich *RNR1* transcript.

Figure 1

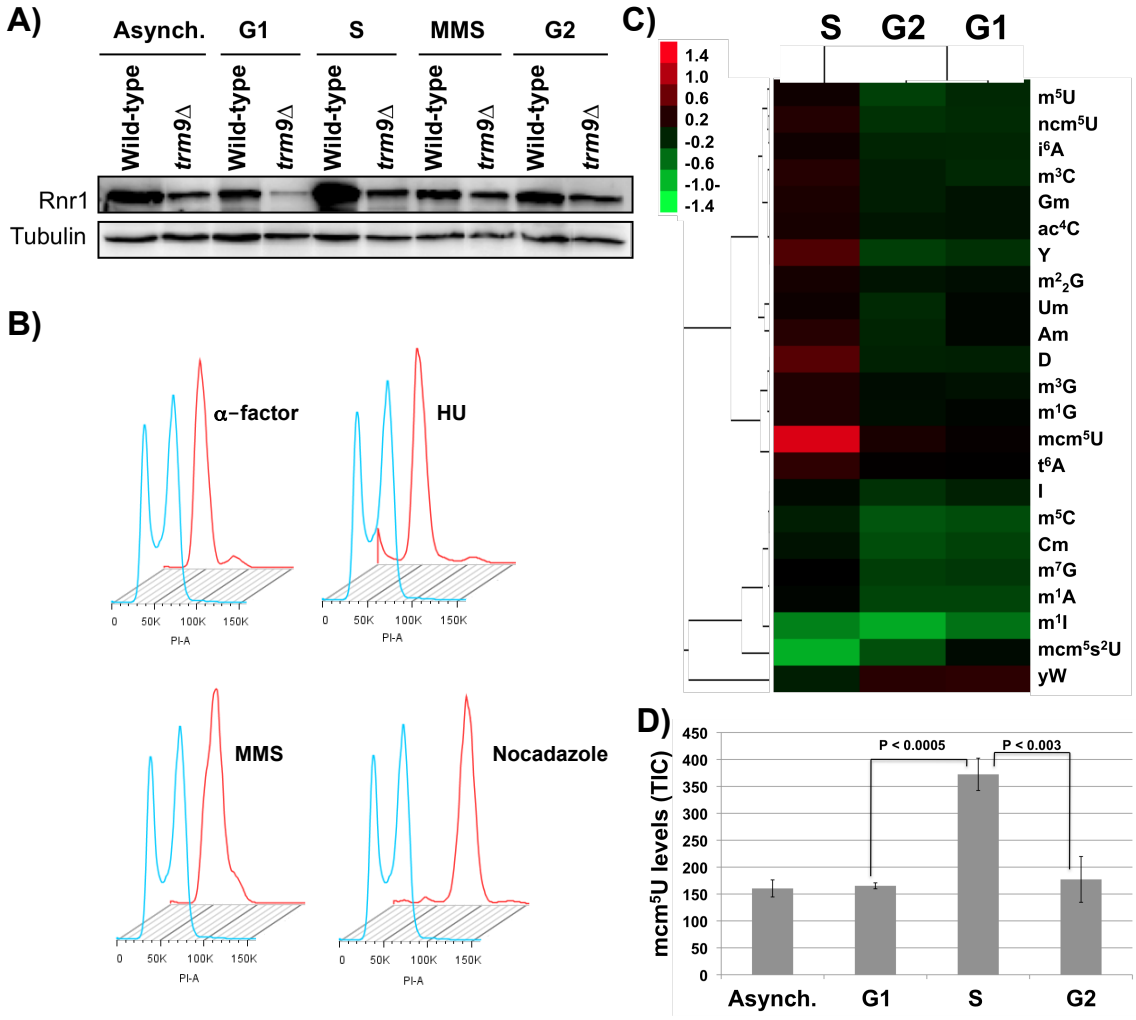
A)
Asynch.
G1
S
MMS
G2
Wild-type
trm9Δ
Rnr1
Tubulin
B)
α−factor
HU
MMS
Nocadazole
0
50K
100K
150K
PI-A
C)
S
G2
G1
1.4
1.0
0.6
0.2
-0.2
-0.6
-1.0-
-1.4
m5U
ncm5U
i6A
m3C
Gm
ac4C
Y
m22G
Um
Am
D
m3G
m1G
mcm5U
t6A
I
m5C
Cm
m7G
m1A
m1I
mcm5s2U
yW
D)
mcm5U levels (TIC)
P < 0.0005
P < 0.003
450
400
350
300
250
200
150
100
50
0
Asynch.
G1
S
G2

Figure 2

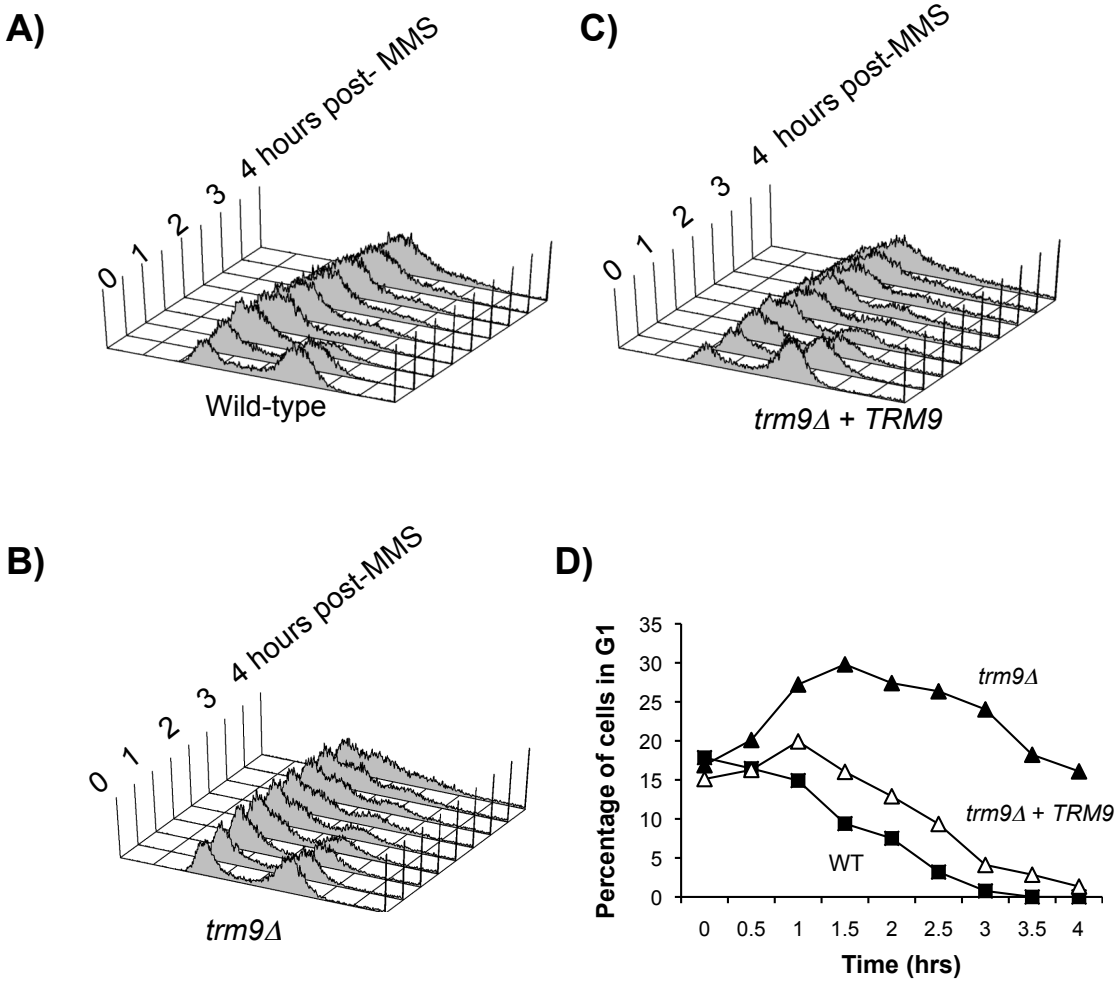
A)
4 hours post- MMS
0
1
2
3
Wild-type
C)
4 hours post-MMS
0
1
2
3
trm9Δ + TRM9
B)
4 hours post-MMS
0
1
2
3
trm9Δ
D)
Percentage of cells in G1
35
30
25
20
15
10
5
0
trm9Δ
trm9Δ + TRM9
WT
0
0.5
1
1.5
2
2.5
3
3.5
4
Time (hrs)

Figure 3

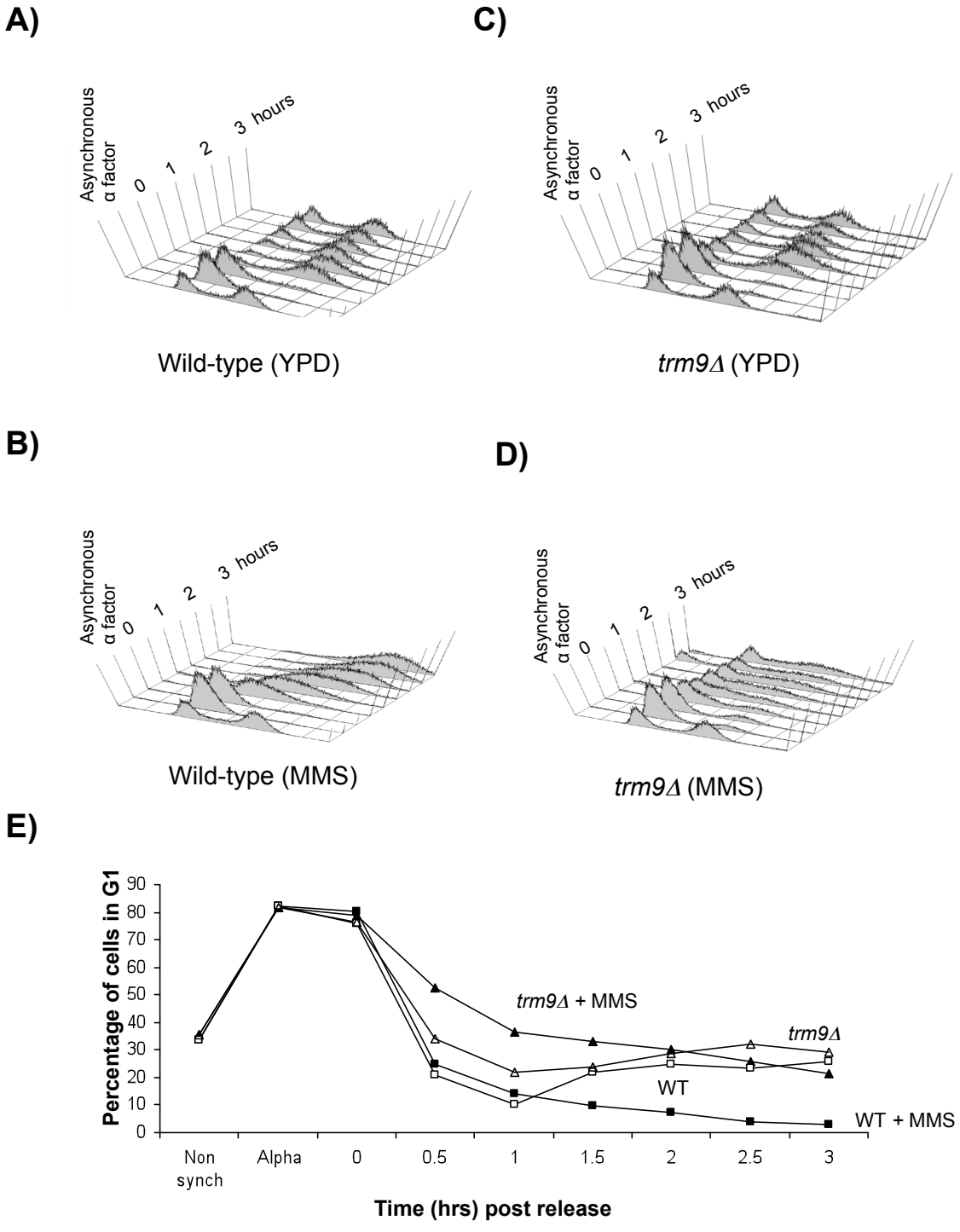
A)
Asynchronous
α factor
0
1
2
3 hours
Wild-type (YPD)
C)
Asynchronous
α factor
0
1
2
3 hours
trm9Δ (YPD)
B)
Asynchronous
α factor
0
1
2
3 hours
Wild-type (MMS)
D)
Asynchronous
α factor
0
1
2
3 hours
trm9Δ (MMS)
E)
Percentage of cells in G1
90
80
70
60
50
40
30
20
10
0
trm9Δ + MMS
trm9Δ
WT
WT + MMS
Non synch
Alpha
0
0.5
1
1.5
2
2.5
3
Time (hrs) post release

Figure 4

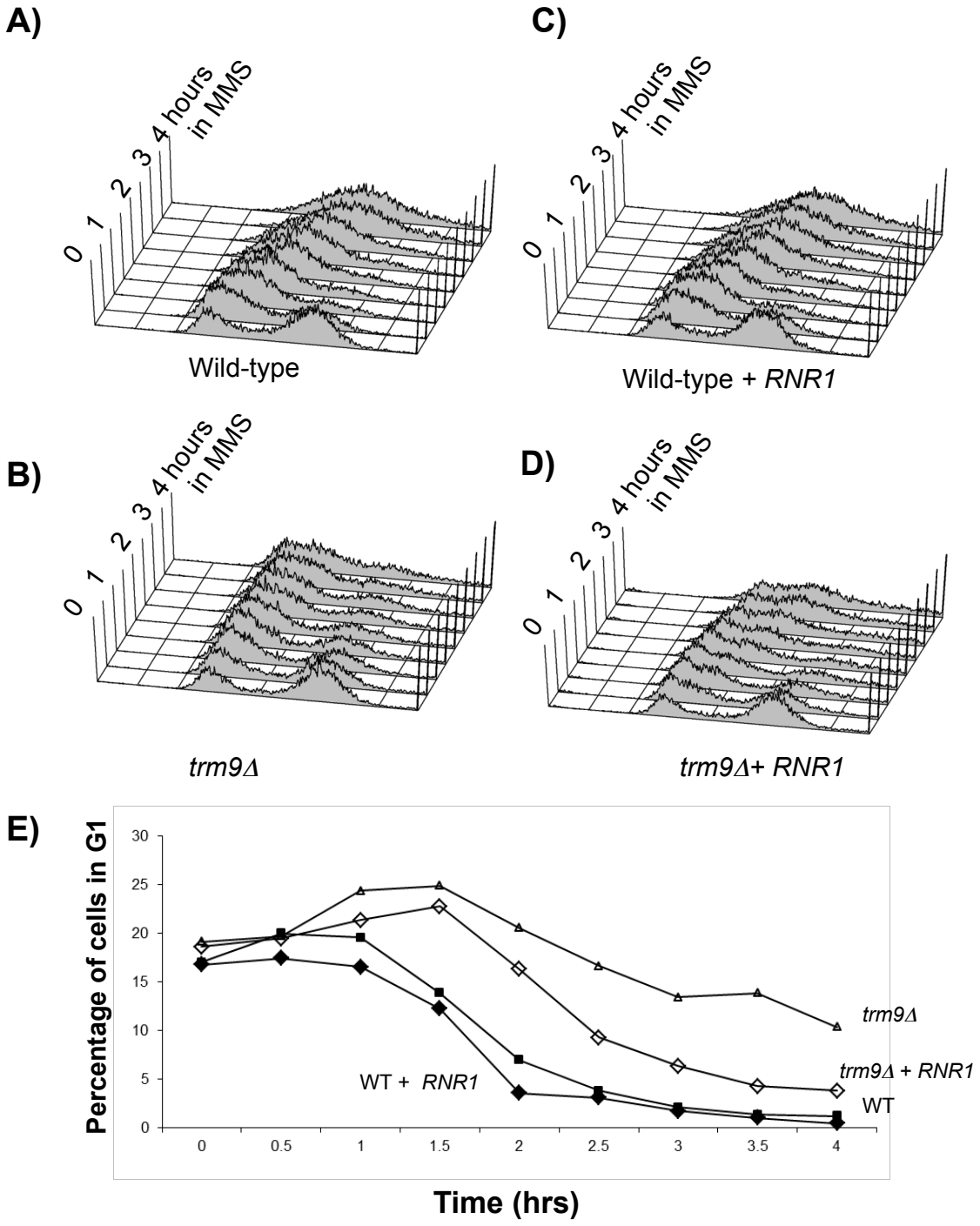
A)
4 hours in MMS
3
2
1
0
Wild-type
C)
4 hours in MMS
3
2
1
0
Wild-type + RNR1
B)
4 hours in MMS
3
2
1
0
trm9Δ
D)
4 hours in MMS
3
2
1
0
trm9Δ+ RNR1
E)
Percentage of cells in G1
30
25
20
15
10
5
0
0
0.5
1
1.5
2
2.5
3
3.5
4
trm9Δ
trm9Δ + RNR1
WT
WT + RNR1
Time (hrs)

Figure 5

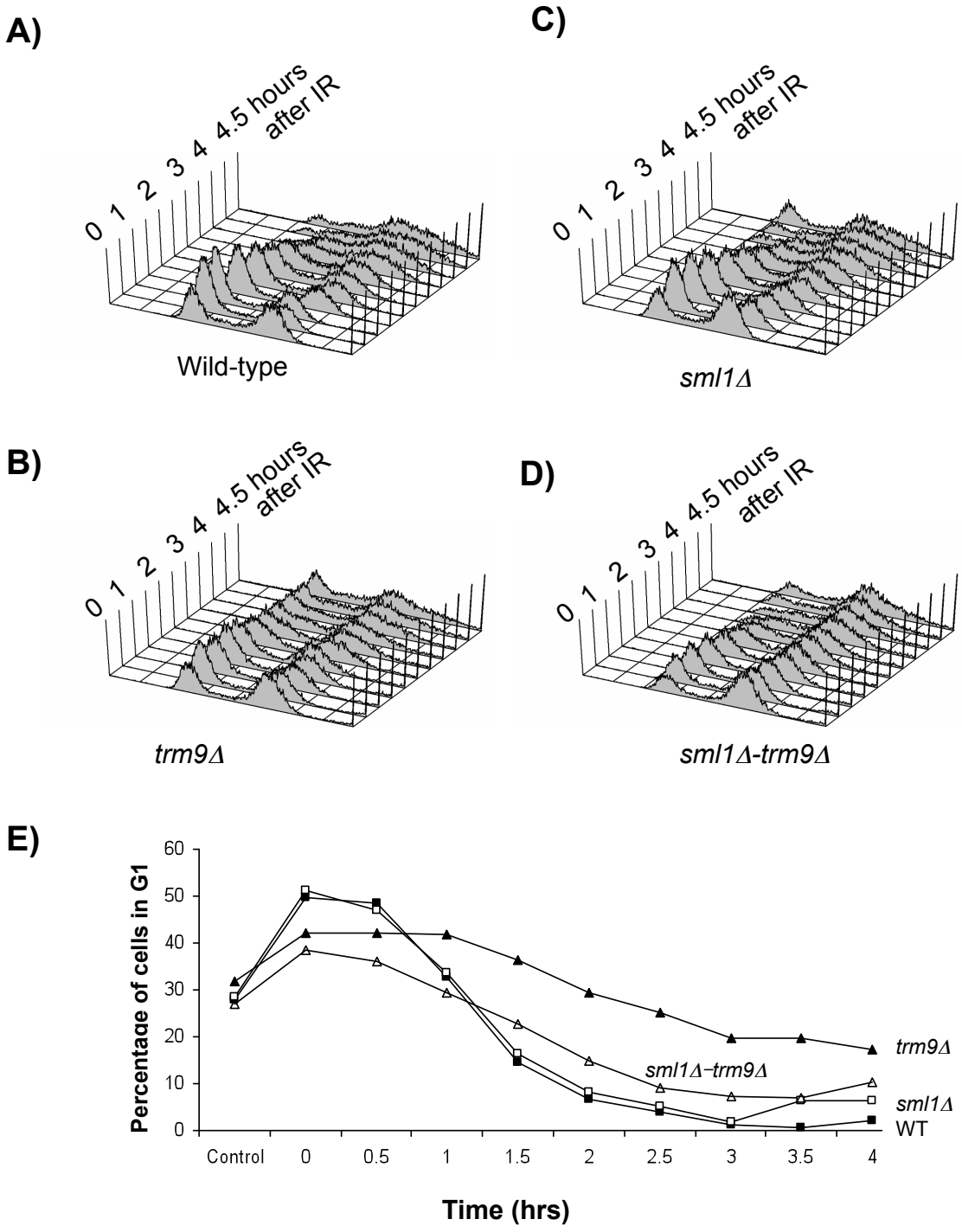
A)
C)
B)
D)
E)
0 1 2 3 4 4.5 hours after IR
Wild-type
sml1Δ
trm9Δ
sml1Δ-trm9Δ
Percentage of cells in G1
60
50
40
30
20
10
0
Control
0
0.5
1
1.5
2
2.5
3
3.5
4
Time (hrs)
trm9Δ
sml1Δ-trm9Δ
sml1Δ
WT

Figure 6

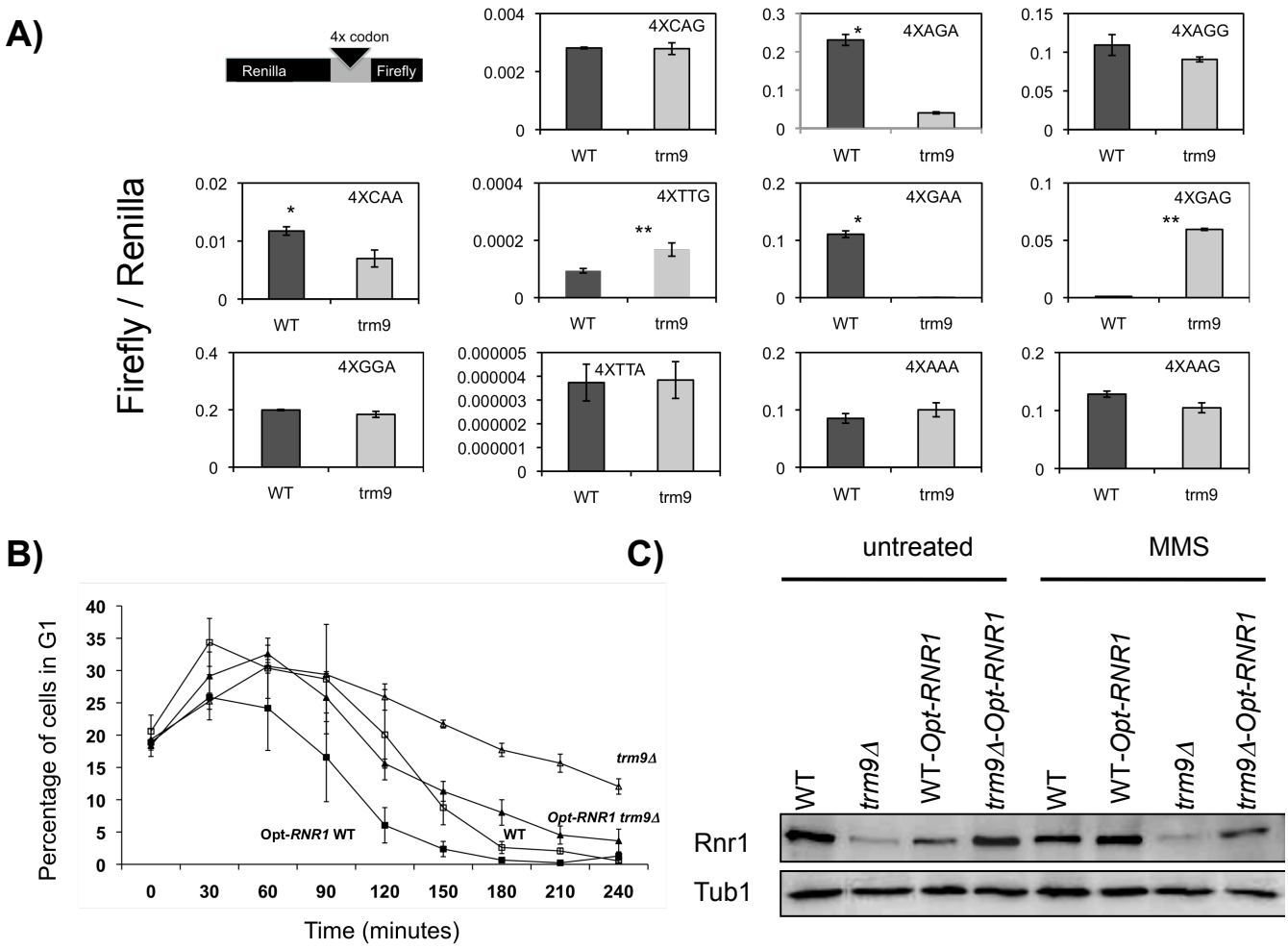
A)
4x codon
Renilla
Firefly
Firefly / Renilla
4XCAG
4XAGA
4XAGG
4XCAA
4XTTG
4XGAA
4XGAG
4XGGA
4XTTA
4XAAA
4XAAG
WT
trm9
B)
Percentage of cells in G1
Time (minutes)
trm9Δ
Opt-RNR1 trm9Δ
Opt-RNR1 WT
WT
C)
untreated
MMS
WT
trm9Δ
WT-Opt-RNR1
trm9Δ-Opt-RNR1
Rnr1
Tub1

Figure 7

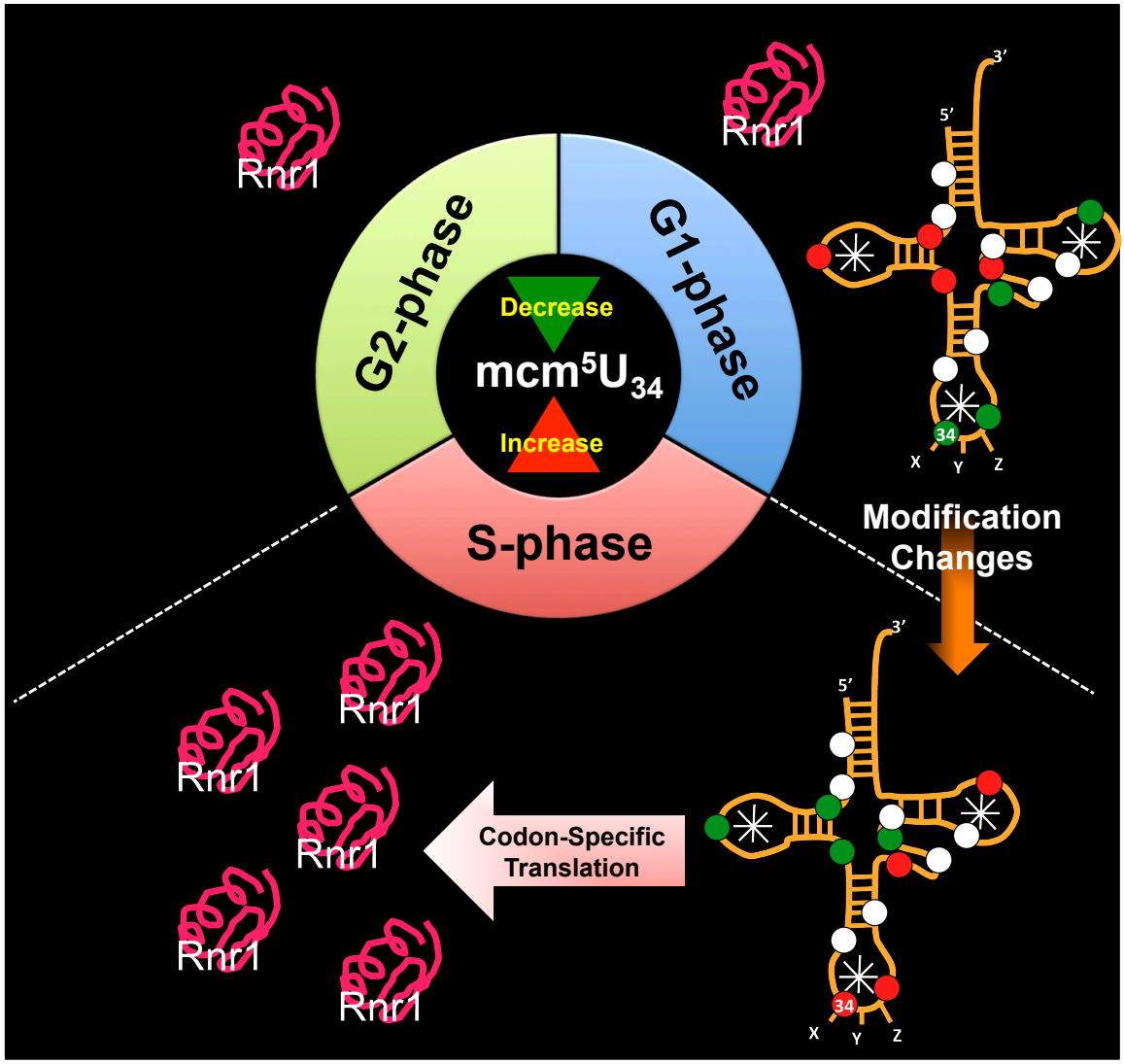
Rnr1
Rnr1
G2-phase
G1-phase
Decrease
mcm5U34
Increase
S-phase
3′
5′
34
X
Y
Z
Modification Changes
Rnr1
Rnr1
Rnr1
Rnr1
Rnr1
Codon-Specific Translation
3′
5′
34
X
Y
Z